A Replication Study of Transfer Learning with Informative Priors: Simple Baselines Better than Previously Reported

Anonymous authors
Paper under double-blind review

Abstract

We pursue transfer learning to improve classifier accuracy on a target task with few labeled examples available for training. Recent work suggests that using a source task to learn a prior distribution over neural net weights, not just an initialization, can boost target task performance by a remarkable 5-10 percentage points. We perform a replication study with careful hyperparameter tuning of all methods on every dataset. We find that standard transfer learning informed by an initialization only performs far better than reported in previous comparisons. Across four datasets and multiple target set sizes, we cannot find a setting where MAP estimation with informative priors improves by 3 or more percentage points over standard transfer learning. Further analysis suggests that the mechanistic justification for informed priors – hypothesized improved alignment between train and test loss landscapes – is not consistently supported due to high variability in empirical landscapes. We release code to allow independent reproduction of all experiments.

1 Introduction

Dataset size is often the limiting factor defining the ceiling of performance in a deep learning application. Without a large dataset of labeled examples available for training, deep learning models face challenges like overfitting and poor generalization (Brigato & Iocchi, 2021). One motivating application with such challenges is medical image classification, especially when labels correspond to diagnoses or annotations obtained by manual review of expert clinicians. In such scenarios, obtaining labels can be prohibitively expensive, and thus often only a small labeled dataset is available (say a few dozen or few hundred examples). Finding other potential sources of information to guide learning can be critical to boost performance.

The field of *transfer learning* offers a promising remedy (Zhuang et al., 2020). The idea is that in addition to a small labeled set for a target task of interest, the user has access to a much larger labeled dataset from a "source" task, such as the well-known ImageNet dataset (Deng et al., 2009). Alternatively, users may have access to a pre-trained model snapshot or distribution derived from such a source. In modern deep learning, the typical off-the-shelf way to benefit from the source task unfolds in two steps. First, obtain a point estimate of neural network weights via "pre-training" on source data. Next, use that point estimate as an initialization for supervised training of the same architecture on the target task, known as "fine-tuning". Throughout, we refer to this two-step process as *standard transfer learning*.

Methods that can deliver further accuracy gains beyond standard transfer learning are naturally of interest to practitioners. Recent results from a new Bayesian transfer learning approach by Shwartz-Ziv et al. (2022) are particularly exciting. Their approach claims to improve upon standard transfer learning by using the source task to learn a distribution over network weights, not just a point estimate for initialization. This distribution then serves as an *informative prior* for the target task. For the target task of classification on CIFAR-10 data given a training set of just 1000 samples, Shwartz-Ziv et al. (2022) report that their maximum a-posteriori (MAP) objective yields an error rate of 27% compared to the 36% possible with standard transfer learning, a gain in accuracy of 9 percentage points. Similar large gains from MAP with informative priors are reported on other datasets when the target training set size n remains rather small ($n \leq 1000$). Beyond MAP point estimation, they report even further gains from Bayesian estimation of the posterior distribution over weights on the target task via stochastic gradient Hamiltonian Monte Carlo (SGHMC) (Chen et al., 2014).

Excited by the reported gains in the simpler MAP setting, our team undertook an extensive investigation into MAP transfer learning with informative priors. We originally intended to quantify how well the gains that Shwartz-Ziv et al. report on natural image datasets transferred to medical imaging scenarios. However, to our surprise our experiments suggest that **standard transfer learning performs better than previously reported** by Shwartz-Ziv et al. (2022). In systematic experiments that vary the size of the target dataset across two natural image datasets and one medical image dataset from dermatology, we find little to no improvement for MAP with informative priors over standard transfer learning in most settings.

Overall, this paper contributes three findings to the study of transfer learning for point estimated weights:

- First, standard transfer learning without any informative prior performs better than reported in Shwartz-Ziv et al. (2022). In the specific setting of CIFAR-10 with 1000 labeled examples for training and a ResNet-50 architecture (He et al., 2016), we find this method hits test set accuracy between 78-82% across multiple replicate samples of the desired training set size, far better than the 64% accuracy (36% error rate) previously reported. This finding is further supported by third-party experiments in Kaplun et al. (2023), who like us reach accuracy near 80% with a similar architecture in the same setting. Large gains over previous reports are also seen at the $n = 100$ setting (see Fig. 1).

- Second, we come to new conclusions about the relative rankings of MAP estimation methods for transfer learning. We find that methods using informative priors perform slightly better than standard initialization-only transfer learning but never by a substantial margin (by 3 or more percentage points). Between methods using informative priors, Shwartz-Ziv et al. (2022)'s low-rank covariance performs better than Chelba & Acero (2006)'s isotropic covariance at small dataset sizes (10 to 100 images per class). However, as dataset size grows, there is no clear winner between methods using informative priors.

- Finally, we empirically assess a specific mechanistic hypothesis from Shwartz-Ziv et al. (2022), who suggest informative priors allow improved "alignment" between the train and test loss landscape of the target fine-tuning task. See an idealized illustration in their Figure 1. We find that on real datasets, informative priors do not often align train and test losses well; instead as shown in our Fig. 2 there is considerable variability in the alignment especially across samples of a small labeled set from the target task.

To take steps to make our present analysis reproducible (including all dataset splitting and hyperparameter tuning procedures), we release a codebase[1] that can re-run all experiments and reproduce all figures here. In the spirit of open science, we welcome any feedback or questions from users.

Our inability to reproduce previously reported results is part of a larger trend across machine learning research (Pineau et al., 2021). We hope our work here helps the community move toward improved best practices. The first best practice we advocate is sharing scripts that enable all experiments, especially those related to hyperparameter tuning. The second best practice is allowing all baselines at minimum the same hyperparameter tuning as a presented method in every experimental setting.

2 Background

Bayesian transfer learning. Recent work by Shwartz-Ziv et al. (2022) proposed Bayesian transfer learning, where a re-scaled posterior from the source task is used as the prior for the target task. This work is motivated by sequential Bayesian updating, where some source data $\mathcal{D}_S$ is acquired, a posterior $p(w|\mathcal{D}_S)$ over weights w is formed, and this posterior is used as an *informed prior* for a target dataset $\mathcal{D}_T$ (Murphy, 2012)

$$p(w|\mathcal{D}_S) \propto p(\mathcal{D}_S|w)p(w) \tag{1}$$
$$p(w|\mathcal{D}_T, \mathcal{D}_S) \propto p(\mathcal{D}_T|w)p(w|\mathcal{D}_S).$$

In sequential Bayesian updating, analysts often assume all data is independent and identically distributed, at least when conditioned on parameters w. However, in transfer learning the target data comes from a

[1] Code: https://anonymous.4open.science/r/bdl-transfer-learning-5327

Table 1: Possible methods for point estimation of neural network weights for a target task. All can be seen as MAP estimation for model defined by a common likelihood and a method-specific prior. The MAP objective is then optimized by first-order stochastic gradient descent. Our work focuses specifically on methods informed by a source task (ImageNet classification), using values of weight vector μ and low-rank (LR) covariance matrix Σ *learned* from this pre-training phase. We include columns for related works and mark the methods they investigate.

Method	**also known as**	**Prior**	**Init.**	**Shwartz-Ziv et al. (2022)**	**Špendl & Pirc (2023)**	**ours**
StdPrior fromScratch	SGD Non-Learned Prior in Shwartz-Ziv et al.	$\mathcal{N}(0, \lambda I)$	random	✓	✓	✗
StdPrior fromImgNet	SGD Transfer Init in Shwartz-Ziv et al.	$\mathcal{N}(0, \lambda I)$	μ	✓	✗	✓
LearnedPriorIso fromImgNet	MAP adaptation in Chelba & Acero	$\mathcal{N}(\mu, \lambda I)$	μ	✗	✗	✓
LearnedPriorLR fromImgNet	SGD Learned Prior in Shwartz-Ziv et al.	$\mathcal{N}(\mu, \lambda \Sigma)$	μ	✓	✓	✓

somewhat different distribution than the source data, so beliefs about which weights are a-priori plausible may need adjustment. To rectify this problem, Shwartz-Ziv et al. (2022) introduce a scaling factor $\lambda \geq 1$ controlling influence of the source-informed prior over weights w. Concretely, λ rescales the covariance matrix of the posterior $p(w|\mathcal{D}_S)$ to form the source-informed prior. When $\lambda = 1$, the model directly uses the source posterior as the source-informed prior. As λ grows larger, the source-informed prior has inflated covariance. In the limit as $\lambda \to \infty$ the influence of the source data disappears (the prior approaches a uniform distribution) and the only influence of the source task on the target task would come from initialization, thus recovering standard transfer learning.

2.1 Common framework for MAP transfer learning.

Probabilistic model for target task. Following Shwartz-Ziv et al. (2022), we form a model that performs a desired target task of image classification with C possible classes. The model has two parts: a backbone and a classification head. Let f denote the backbone neural network with weights $w \in \mathbb{R}^d$. For modern computer vision, d might be in the millions or even billions. Given an image x_i of prespecified size, f produces a hidden representation vector $f_w(x_i) \in \mathbb{R}^H$. We assume the first entry of this vector is always 1 to allow learning intercepts. Define the classifier head as parameterized by weights $V \in \mathbb{R}^{C \times H}$ that can map the representation vector to logits over C classes. Then, given a target training set of size n, containing pairs $\{x_i, y_i\}_{i=1}^n$ of images x_i and categorical labels $y_i \in \{1, 2, \dots C\}$, we have the following **template** for a probabilistic model:

$$p(w) = \mathcal{N}(w \mid \mathbf{m}, \lambda \mathbf{S}) \qquad \text{source-informed prior on backbone} \tag{2}$$

$$p(V) = \mathcal{N}(\text{vec}(V) \mid 0, \tau I), \qquad \text{prior on clf. head} \tag{3}$$

$$p(y_{1:n}|V, w) = \prod_{i=1}^{n} \text{Cat}\big(y_n|\text{softmax}(V f_w(x_i))\big) \qquad \text{likelihood} \tag{4}$$

Here, $\tau > 0$ and $\lambda > 0$ are key hyperparameters that require tuning, while the choice of $\mathbf{m}, \mathbf{S}$ is method specific; these values may be simple (e.g. an all-zero mean) or informed by a source-task.

Target task MAP estimation. We can fit the above model to the target dataset via a MAP point estimation strategy, finding values of weights w, V that minimize the objective

$$L(w, V) := -\frac{1}{n}\Big[\sum_{i=1}^{n} \log p(y_i|V, w) + \log p(V) + \log p(w)\Big] \tag{5}$$

Given a concrete target dataset, we pursue stochastic first-order gradient descent to obtain estimates of w, V. In transfer learning, it is common to initialize backbone weights w at a known good value from the source task, denoted μ. Head weights V can be initialized randomly.

As surveyed below, several approaches to transfer learning in the literature share both the common model template defined above and the pursuit of MAP estimation. They vary only in the setting of the backbone prior's mean vector $\mathbf{m}$ and covariance matrix $\mathbf{S}$. Tab. 1 summarizes the specific possible methods.

2.2 Concrete methods for MAP transfer learning.

Below we cover a spectrum of possible choices for the prior over backbone weights, all of which can be integrated into the common MAP transfer learning framework above. They differ in whether and how the prior is informed by a source task, especially the source-informed point estimate μ of the backbone weights.

Standard non-informed isotropic prior. The *standard* transfer learning approach most common in the literature is to set $\mathbf{m}$ to the all zero vector and set $\mathbf{S}$ to the identity matrix. We refer to this as *StdPrior* throughout (read as "standard prior"). Here, the backbone prior is not informed by the source task; the only source-informed knowledge comes from initializing MAP estimation at source-informed weights μ.

Learned prior with isotropic covariance. A natural way to let the source task inform the backbone prior is to set the mean such that $\mathbf{m} = \mu$. The prior covariance $\mathbf{S}$ is left as the identity matrix. This corresponds to an older method from Chelba & Acero (2006), known as *MAP adaptation*, which was recommended as the "standard baseline for solving transfer learning tasks and benchmarking new algorithms" in Xuhong et al. (2018). We refer to this as *LearnedPriorIso* throughout.

Learned prior with low-rank (LR) covariance. Shwartz-Ziv et al. (2022) propose informing both the prior's mean and covariance matrix from the source task. They use Stochastic Weight Averaging-Gaussian (SWAG) (Maddox et al., 2019) to approximate the posterior distribution $p(w|\mathcal{D}_S)$ of the source data $\mathcal{D}_S$ with a Gaussian distribution as $\mathcal{N}(\mu, \Sigma)$ where μ is the learned mean and $\Sigma = \frac{1}{2}(\Sigma_{\text{diag}} + \Sigma_{\text{LR}})$ is a *low-rank* representation of a covariance matrix. For a d-parameter neural net with typical d in millions or billions, a standard $d \times d$ covariance matrix is unaffordable to store. Thus, we select a concrete desired rank k (where $k \ll d$), and form the LR covariance as $\Sigma_{\text{LR}} = \frac{1}{k-1} QQ^T$, where $Q \in \mathbb{R}^{d \times k}$ is a learned parameter from the source task. We refer to this as *LearnedPriorLR* throughout, and use $k = 5$ throughout as recommended by Shwartz-Ziv et al..

2.3 Previous replication efforts with informative priors.

Work on informative priors by Shwartz-Ziv et al. (2022) has generated considerable follow-up attention, including a previous replication study with different goals than ours. Špendl & Pirc (2023) sought to compare "from scratch" training on the target task alone (without even a source-informed initialization) to the proposed informed prior MAP procedure. Špendl & Pirc (2023) used Shwartz-Ziv et al. (2022)'s released code with a fixed initial learning rate and weight decay on just one dataset (Oxford Flowers-102 dataset by Nilsback & Zisserman (2008)). They report that transfer learning with informed priors did outperform a simple from-scratch baseline that did not do *any* transfer from source to target (see Tab. 1 for a comparison of which methods all papers investigate). In contrast, we run experiments designed to compare standard initialization-only transfer learning to informed prior transfer learning. Our experiments also perform separate hyperparameter tuning for all methods at all dataset sizes.

Looking closely at results from Špendl & Pirc (2023), we note one interesting finding in common with our work. In a sensitivity study of the covariance scaling factor λ, they find that setting it extremely large (to 10^9, the highest value attempted) improved the performance of the informative-prior method. We suggest this should be interpreted as making the prior close-to-uniform, supporting our later experiments that suggest the primary value of the source task in transfer learning is from initialization, not a learned prior.

3 Experimental Procedures

We seek to fairly compare three distinct methods for point estimating optimal neural network weights w, V for a target classification task. All three make use of pre-training on a source task, some via initialization only and some via an additional learned prior, as described in Sec. 2.2 and summarized in Table 1. We refer to these methods in all result tables and figures as *StdPrior* for standard transfer learning with an uninformative standard Gaussian prior with zero mean and isotropic covariance $\mathbf{S}{=}\lambda I$, *LearnedPriorIso* for a source-informed prior with learned mean μ but isotropic covariance $\mathbf{S}{=}\lambda I$, and *LearnedPriorLR* for the source-informed prior with mean μ and learned low-rank covariance multiplied by scalar λ.

Below we provide essential details of our experimental procedure. We intend that all experiments are fully reproducible by others. See Tab. B.1 in App. B for a detailed comparison of Shwartz-Ziv et al. (2022)'s and our experimental procedures. For further details, see App. A as well as our released codebase.

Datasets and classification tasks. We study targeted classification tasks from four distinct open-access datasets. For all tasks, we study how well variants of MAP estimation can *transfer* knowledge from a source task on ImageNet.

The first two datasets were selected as common benchmarks that enable direct comparisons to previous experiments by Shwartz-Ziv et al. (2022): the 10-way classification task of CIFAR-10 (Krizhevsky et al., 2010), the 102-way classification task of Oxford Flowers (Nilsback & Zisserman, 2008), and the 37-way classification task of Oxford-IIIT Pets (Parkhi et al., 2012). Each of these contains natural images (RGB, resized to 224x224 pixels) that typically depict one object of the labeled class.

For the last dataset, we select HAM10000 (Tschandl et al., 2018; Codella et al., 2019), an open-source deidentified dataset, informally known as "Skin Cancer MNIST", designed to support assessment of automatic diagnosis of several possible skin lesion types from RGB images resized to 224x224 pixels of skin surface microscopy (dermatoscopy). To avoid extreme imbalance, we form a 4-class classification task between 3 original classes with sufficient data (at least 10% prevalence) and an additional "other" class that combines all other original classes.

Common architecture and optimization. Across all experiments, we always set the backbone architecture of network f to a ResNet-50 (He et al., 2016). This directly matches the experiments in Shwartz-Ziv et al. (2022). Our PyTorch-based codebase uses a common optimization procedure for training: SGD with batch size of 128 and Nesterov momentum of 0.9 with cosine-annealing schedule for learning rate (Loshchilov & Hutter, 2016). Initial learning rate is a tuned hyperparameter (see below).

Common source-task knowledge. For all methods, we take the learned weights μ that form the initialization (and if needed, the prior mean), from Shwartz-Ziv et al. (2022)'s released snapshots[2]. For *LearnedPriorLR*, we also obtain the diagonal and low-rank ingredients for the covariance matrix directly from Shwartz-Ziv et al. (2022)'s released snapshots. We specifically use Shwartz-Ziv et al.'s snapshots pre-trained on ImageNet with SimCLR (Chen et al., 2020), following their recommendation that pre-training with self-supervised learning (as in SimCLR) leads to improved transfer learning compared with fully-supervised learning (e.g. using cross-entropy loss with ImageNet class labels).

Varying train set size n. For each dataset, we setup a range of transfer learning tasks by artificially varying n, the number of available samples for training. In all cases, we ensure *balanced class frequencies*, ensuring the same number of images per class. For CIFAR-10, by selecting $n \in \{10, 100, 1000, 10000, 50000\}$, we cover exactly 1, 10, 100, 1000, and all available examples per class. For Oxford Flowers, we select $n \in \{102, 510, 1020\}$ to cover 1, 5, and 10 examples per class. For Oxford-IIIT Pets, we select $n \in \{37, 370, 3441\}$ to cover 1, 10, and 93 examples per class (93 is the maximum possible value that keeps exact balance). For HAM10000, we select $n \in \{100, 1000\}$. We emphasize that the 10-1000 examples per class regime is likely of most practical interest for many applications.

Repeated trials. At each chosen value of n, we build 3 separate "replicate" training sets by randomly sampling n image-label pairs from the predefined complete training set (without replacement). We then separately perform all training (including hyperparameter tuning) on each replicate. We emphasize we are careful to ensure similar class-composition for all replicates.

Hyperparameter tuning. All methods need to tune three key hyperparameters: the covariance scaling factor λ, the classification head weight decay τ, and the initial learning rate. To give informative prior approaches the best possible settings, for *LearnedPriorLR* we tune all three together. For simplicity, for both *StdPrior* and *LearnedPriorIso* we fix $\lambda = \tau$, tuning only τ and learning rate. In some ways, this setup puts standard transfer learning at a disadvantage, as *LearnedPriorLR* is allowed to search a larger hyperparameter space.

Model fitting (including tuning) has two stages. In the first stage, we first randomly divide available data of size n into a train set and validation set with 4:1 ratio. We then tune all hyperparameters via grid search (ranges in App. A.2), selecting the best configuration based on the log likelihood of the labels of the validation set. After selecting an optimal hyperparameter configuration in stage one, we refit to the entire dataset of

[2]Shwartz-Ziv et al. (2022)'s SimCLR snapshots can be found at `https://github.com/hsouri/BayesianTransferLearning`

n examples in stage two. In all stages, the optimizer runs until reaching a specified maximum number of iterations.

Performance metrics on test set. All datasets provide a predefined train/test split which our experiments respect. We report heldout performance metrics on the complete available test set for each task. For CIFAR-10, Oxford Flowers, and Oxford-IIIT Pets, we report *classifier accuracy* (higher is better) following Shwartz-Ziv et al. (2022). For HAM10000, we report *average AUROC* (higher is better), macro-averaged over all classes. Ultimately, we report the average performance metric across all 3 replicate trials, as well as the min-max range. For all tasks, we also assess the *negative log likelihood* (NLL) of the test set.

4 Results

Examining the results of all experiments, we come to three key findings. These are detailed in the subsections below.

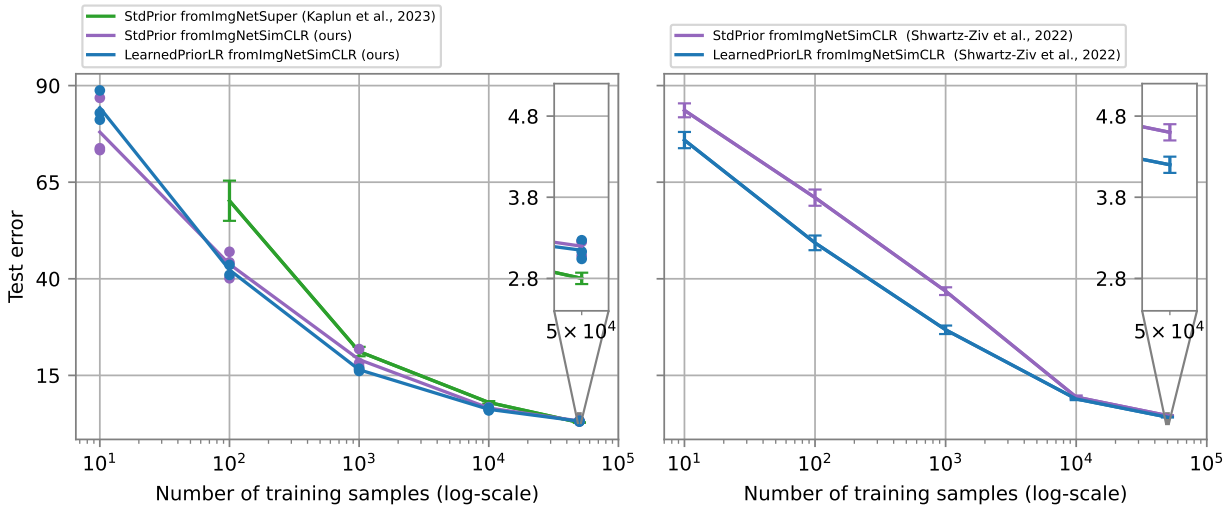

Figure 1: Error rate (lower is better) vs. target train set size on CIFAR-10, for various MAP estimation methods for transfer learning from ImageNet. *Left:* Our results. *Right:* Results copied from Shwartz-Ziv et al. (2022) (their Tab. 10). **Takeaway: In our experiments, standard transfer learning does better than previously reported.** *Setting details:* The blue and purple lines across both panels come from comparable settings: a common ResNet-50 architecture and common learned values for mean and low-rank (LR) covariance taken directly from the SimCLR pre-trained snapshots in Shwartz-Ziv et al. (2022)'s repository. *Green line:* The left panel's green line is a third-party experiment copied from Kaplun et al. (2023), suggesting others can achieve similar performance as we do for standard transfer learning with ResNet-50. They use fully-supervised pre-training not self-supervised SimCLR. Plotted mean and standard deviations confirmed via direct correspondence with Kaplun et al..

4.1 Finding 1: Standard transfer learning better than reported in Shwartz-Ziv et al. (2022).

Our Fig. 1 provides a side-by-side comparison of results on CIFAR-10 for our experiments (left) compared to those originally reported in Shwartz-Ziv et al. (2022) (right). Here, we report error rate (lower is better) and use a color scheme that matches original plots from Shwartz-Ziv et al.. We see that *StdPrior* (purple line) is consistently 10-15 percentage points better at dataset sizes $n \in \{100, 1000\}$, essentially erasing the gap in performance previously attributed to informative priors.

Our results are further supported by other third-party experiments by Kaplun et al. (2023) that use the same architecture (ResNet-50) and same source task (ImageNet) to classify CIFAR-10. Our results at $n = 1000$ show test error for *StdPrior* in the 17-22% range, matching results from Kaplun et al. (green line in our figure) well. We suggest this lends credibility to our claim that it is possible for others to do far better with standard transfer learning than has been previously reported. We note that Kaplun et al. do pre-training with supervised methods, not the self-supervised SimCLR; see App. D for a comparison with Shwartz-Ziv et al. (2022)'s fully-supervised pre-training results.

Table 2: CIFAR-10 heldout accuracy (higher is better) as target train set size n increases. For each method and train set size n, we ran our two-phase training pipeline (including hyperparameter tuning) on 3 distinct training sets (independent samples of n examples from the provided full training set). We report mean accuracy on test set across these 3 trials, along with the min-max range. 10 classes, balanced. See App. A for details.

Method	n = **10**	**100**	**1000**	**10000**	**50000**
StdPrior fromImgNet	22.0 (13.2-26.7)	56.2 (53.0-59.9)	80.9 (78.2-82.8)	93.4 (93.3-93.7)	96.8 (96.7-96.9)
LearnedPriorIso fromImgNet	20.7 (17.7-23.4)	56.7 (54.8-59.8)	81.9 (81.6-82.1)	94.3 (94.1-94.5)	97.3 (97.2-97.4)
LearnedPriorLR fromImgNet	15.7 (11.3-18.8)	58.7 (56.4-60.6)	83.5 (83.3-83.9)	93.8 (93.4-94.1)	96.9 (96.7-97.0)

Table 3: Oxford Flowers heldout accuracy (higher is better) as target train set size n increases. For each method and train set size n, we ran our two-phase training pipeline (including hyperparameter tuning) on 3 distinct training sets (independent samples of n examples from the provided full training set). We report mean accuracy on test set across these 3 trials, along with the min-max range. 102 classes, balanced. See App. A for details.

Method	n = **102**	**510**	**1020**
StdPrior fromImgNet	31.1 (12.6-40.6)	78.9 (78.4-79.3)	87.9 (87.4-88.1)
LearnedPriorIso fromImgNet	19.2 (9.0-34.8)	79.1 (78.5-79.4)	88.6 (88.2-89.1)
LearnedPriorLR fromImgNet	28.8 (10.6-39.2)	77.9 (74.8-79.4)	88.4 (88.2-88.7)

Table 4: Oxford-IIIT Pets heldout accuracy (higher is better) as target train set size n increases. For each method and train set size n, we ran our two-phase training pipeline (including hyperparameter tuning) on 3 distinct training sets (independent samples of n examples from the provided full training set). We report mean accuracy on test set across these 3 trials, along with the min-max range. 37 classes, balanced. See App. A for details.

Method	n = **37**	**370**	**3441**
StdPrior fromImgNet	17.3 (14.5-20.0)	54.8 (53.2-57.5)	86.4 (86.0-86.6)
LearnedPriorIso fromImgNet	7.0 (5.4- 8.5)	55.5 (53.3-57.7)	86.4 (85.4-87.0)
LearnedPriorLR fromImgNet	6.6 (6.2- 7.3)	57.4 (56.2-58.2)	86.7 (85.0-87.8)

Table 5: HAM10000 AUROC on heldout data (higher is better, macro-averaged across classes) as target train set size n increases. For each method and size n, we ran our two-phase training (including hyperparameter tuning) on 3 distinct training sets (independent samples of size n from the provided full training set). We report mean AUROC on test set across 3 trials (min-max range). 4 classes, ranging from 11%-67% prevalance. See App. A for details.

Method	n = **100**	**1000**
StdPrior fromImgNet	78.1 (75.0-82.8)	85.6 (85.0-86.3)
LearnedPriorIso fromImgNet	78.0 (75.0-82.8)	86.5 (85.5-87.4)
LearnedPriorLR fromImgNet	78.7 (74.9-82.7)	86.6 (85.0-87.5)

4.2 Finding 2: Methods using informative priors perform slightly better than standard transfer learning.

Ultimate test set performance for all methods across train set sizes n is reported for all 4 datasets in Tables 2, 4, 3, and 5 respectively. Each table entry reports that method's mean test accuracy across the 3 replicate samples of n training points, as well as the min-max range.

Across all tables, in the majority of settings, methods using informative priors perform slightly better than standard transfer learning (except when the training set size equals the number of classes). These consistent performance gains come from our fix to Shwartz-Ziv et al. (2022)'s implementation of rescaling the low-rank covariance matrix (see Tab. B.1 in App. B for details). However, the margins of victory are all less than 3 percentage points, far lower than the 5-10 percentage point gains reported in Shwartz-Ziv et al. (2022) at similar settings.

Between methods using informative priors, there are a few cases where Shwartz-Ziv et al. (2022)'s low-rank covariance is clearly better than Chelba & Acero (2006)'s isotropic covariance: CIFAR-10 at n=100 has 58.7% for *LearnedPriorLR* vs. 56.7% for *LearnedPriorIso*; CIFAR-10 at n=1000 has 83.5% for *LearnedPriorLR* vs. 81.9% for *LearnedPriorIso*; and Oxford-IIIT Pets at n=370 has 57.4% accuracy for *LearnedPriorLR* vs. 55.5% accuracy for *LearnedPriorIso*. However, as dataset size grows, there is no clear winner between methods using informative priors. Examining the two largest training set sizes for CIFAR-10 (where training should be most aligned with the true target task), Shwartz-Ziv et al. (2022)'s low-rank covariance performs worse than an isotropic covariance.

Further results in App. C compare methods using NLL as a performance metric. Again, the conclusion is that there is not a setting where there is a convincing win from informative prior.

4.3 Finding 3: Large variability in quality of alignment between training and test loss landscapes.

Shwartz-Ziv et al. (2022) suggest an underlying mechanism for why informed priors improve transfer learning: better alignment between the loss landscapes of the target classification task across the small available training set and the large test set. (Remember, test set performance is assumed a reliable "gold-standard" here due to its size, but such data is not available for training in the proposed transfer learning setting). See an idealized illustration in their Figure 1, where the overall function shape and especially the locations of minima are far more similar across train and test with source-informed priors than standard methods.

To empirically study this proposed phenomenon, we examine how informed priors reshape the loss surface on the CIFAR-10 task when $n = 1000$. It is difficult to visualize the high-dimensional input space (the size of all weights w is over 23 million), so we look at a 1D slice that linearly interpolates between two values: the optima w^*_{Std} found by *StdPrior* MAP estimation or the optima w^*_{LR} found by *LearnedPriorLR* and the optima w^* found at the largest dataset size. (We interpolate between classifier heads V as well, but use just w symbols for simplicity). Each panel of Fig. 2 visualizes over this 1D interpolation how two functions behave: the train set loss of each MAP objective (red line, vary by columns as *StdPrior* or *LearnedPriorLR*), and the test set NLL (blue, vary by columns as different 1D slices). Each row comes from a different replicate sample of $n = 1000$ image-label pairs for training.

If informed priors lead to better alignment, we contend that this should be visible in these plots: the location of the minima for the blue test curve should be closer to the source-informed optima w^*_{LR} than the standard method optima w^*_{Std}. We label the Euclidean distance in each plot to help readers focus on which method reduces the gap between trained and ideal minimum. However, across 3 replicate train sets (rows) we find there is high variability in how methods rank in alignment. Sometimes, w^*_{LR} does have a smaller gap, indicating better alignment (bottom row). However, we also find the gap can be similar (middle row) or even prefer the standard method (top row). We thus suggest that there is considerable variability in alignment quality, making the empirical evidence for the loss-alignment hypothesis of Shwartz-Ziv et al. (2022) less decisive than their idealized illustration would suggest.

5 Discussion and Conclusion

Identifying the reason our current study leads to different conclusions than prior work is complex. The code released by the original study authors was incredibly useful to us. We are very thankful to the authors for making it available, it was more usable than other code repositories we have seen. However, we found their released code does not allow exact replication of key experimental steps from Shwartz-Ziv et al. (2022), such as replicable sampling of the same n image-label pairs they used for training in their experiments, or how exactly to perform hyperparameter tuning (how to carve out a validation set from available data, etc.). It is thus difficult to isolate what setting in our present study lead to the different results seen here, though we attempt a careful side-by-side comparison in App. B. Our current best guess is that our substantial effort into fair hyperparameter tuning of all methods led to improved numbers for standard transfer learning. We stress that our ultimate goal is to improve the community's shared understanding about how to best achieve the goals of transfer learning, not to cast doubt on others.

Is standard transfer learning better than full Bayesian inference? We stress that all findings are confined to the simpler MAP point estimation setting; we do not study the full Bayesian posterior estimation methods of Shwartz-Ziv et al. (2022), which require notable additional computational complexity across fine-tuning and testing phases of the model development life cycle. For example, fine-tuning is usually at least 5-10x as time-consuming. Full Bayesian approaches also require substantive expertise from downstream practitioners when debugging is needed.

That said, our standard transfer learning results on CIFAR-10 are as good as or better than the full Bayesian inference results reported in Shwartz-Ziv et al. (2022) (for a direct comparison, see our Fig. F.1 in App. F). We expect deep ensembles to improve on our results. We leave it to future work to investigate performance gains from full Bayesian inference.

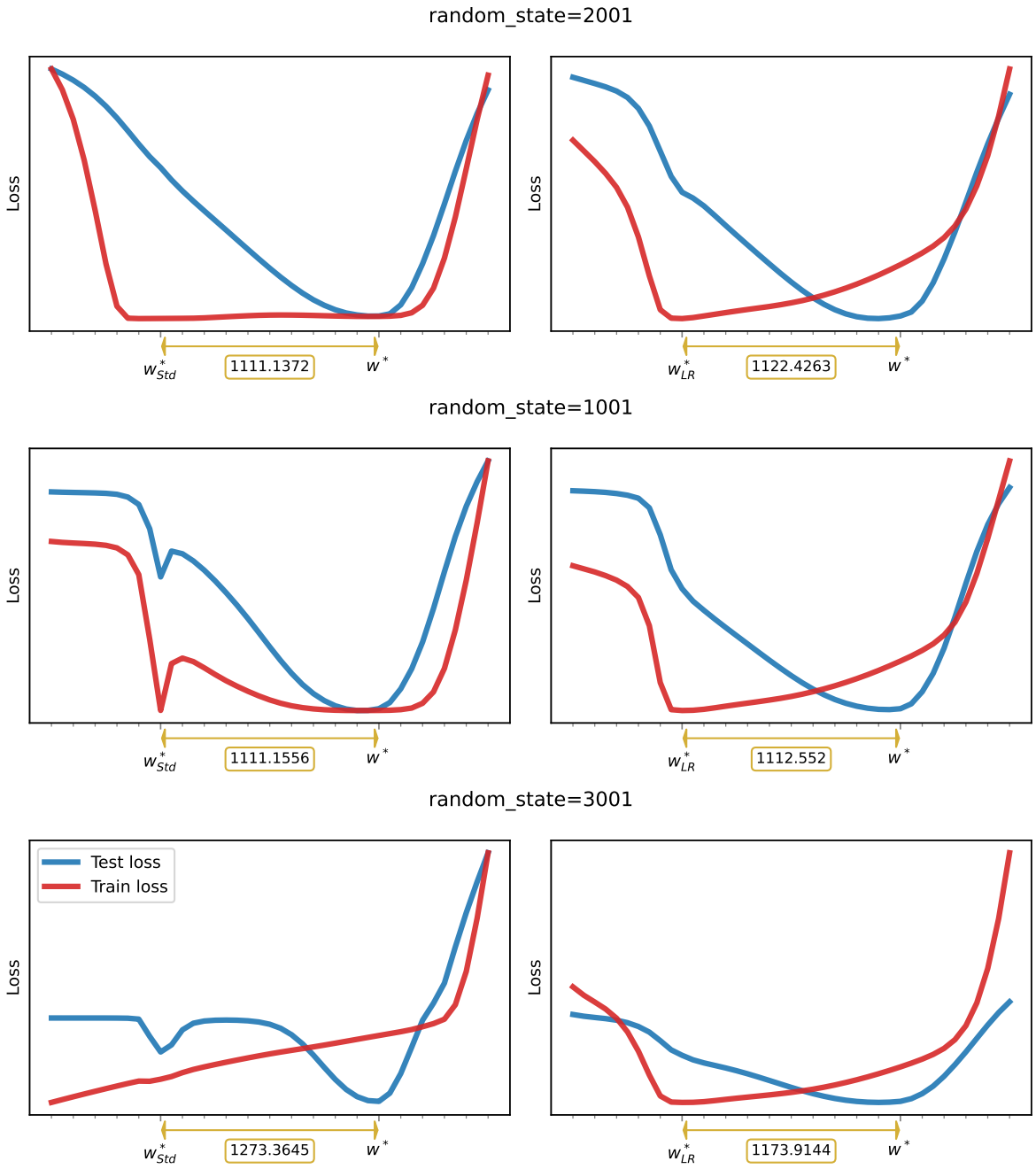

(a) Standard transfer learning (*StdPrior*)

(b) *LearnedPriorLR*

Figure 2: Empirical alignment of loss landscapes for target task across train and test for CIFAR-10 $n = 1000$. Compare to Shwartz-Ziv et al.'s Figure 1, which is an idealized illustration not an empirical result. *Each panel:* We assess a 1D slice of the high-dimensional landscape by linearly interpolating parameters w between the optima w^*_{Std} found via minimizing the standard MAP objective (left) or the optima w^*_{LR} found via minimizing the *LearnedPriorLR* MAP objective (right) and the optima w^* found at the largest dataset size. Red curve shows the indicated training loss (varies by column) on CIFAR-10 with $n = 1000$ samples; blue curve (varies by column) shows CIFAR-10 test set NLL. Each row shows results from a different train set sample of size $n = 1000$. The gap between the optima found via training and the test set's ideal minimum is shown as a double-sided gold arrow. **Takeaway: Shwartz-Ziv et al. (2022)'s learned prior approach does not always reduce the gap between trained and ideal minimum.**

What transfer learning method is recommended? Based off our experiments, when point estimating neural network weights we recommend both *StdPrior* and *LearnedPriorIso* for their simplicity and performance. We do not see enough of a large consistent boost in discriminative performance from Shwartz-Ziv et al. (2022)'s low-rank covariance to clearly justify its downstream use as a "default" approach. However, there are a few cases at small dataset sizes where Shwartz-Ziv et al. (2022)'s low-rank covariance is clearly better than Chelba & Acero (2006)'s isotropic covariance and may be a method to reach for to boost target task performance by a couple percentage points.

Limitations. We only consider transfer learning from one fixed source task, ImageNet. Further work could investigate if informative priors may be more useful if the source task is more directly related to a target task of interest. To define the priors, we also only consider one fixed mean vector and learned low-rank (with rank $k = 5$) covariance matrix taken directly from released snapshots by others. Others could find different behavior with other pre-training procedures, especially with more tuning of the rank on the target task.

References

Lorenzo Brigato and Luca Iocchi. A Close Look at Deep Learning with Small Data. In *2020 25th International Conference on Pattern Recognition (ICPR)*, 2021.

Ciprian Chelba and Alex Acero. Adaptation of Maximum Entropy Capitalizer: Little Data Can Help a Lot. *Computer Speech & Language*, 20(4):382–399, 2006.

Tianqi Chen, Emily Fox, and Carlos Guestrin. Stochastic Gradient Hamiltonian Monte Carlo. In *International Conference on Machine Learning (ICML)*, 2014.

Ting Chen, Simon Kornblith, Mohammad Norouzi, and Geoffrey Hinton. A Simple Framework for Contrastive Learning of Visual Representations. In *International Conference on Machine Learning (ICML)*, 2020.

Noel Codella, Veronica Rotemberg, Philipp Tschandl, M Emre Celebi, Stephen Dusza, David Gutman, Brian Helba, Aadi Kalloo, Konstantinos Liopyris, Michael Marchetti, Harald Kittler, and Allan Halpern. Skin Lesion Analysis Toward Melanoma Detection 2018: A Challenge Hosted by the International Skin Imaging Collaboration (ISIC). *arXiv preprint arXiv:1902.03368*, 2019.

Jia Deng, Wei Dong, Richard Socher, Li-Jia Li, Kai Li, and Li Fei-Fei. ImageNet: A Large-Scale Hierarchical Image Database. In *Proceedings of the IEEE/CVF Conference on Computer Vision and Pattern Recognition (CVPR)*, 2009.

Kaiming He, Xiangyu Zhang, Shaoqing Ren, and Jian Sun. Deep Residual Learning for Image Recognition. In *Proceedings of the IEEE/CVF Conference on Computer Vision and Pattern Recognition (CVPR)*, 2016.

Gal Kaplun, Andrey Gurevich, Tal Swisa, Mazor David, Shai Shalev-Shwartz, and Eran Malach. SubTuning: Efficient Finetuning for Multi-Task Learning. *arXiv preprint arXiv:2302.06354*, 2023.

Alex Krizhevsky, Vinod Nair, and Geoffrey Hinton. CIFAR-10 (Canadian Institute for Advanced Research). 2010. URL http://www.cs.toronto.edu/~kriz/cifar.html.

Ilya Loshchilov and Frank Hutter. SGDR: Stochastic Gradient Descent with Warm Restarts. In *Proceedings of the International Conference on Learning Representations (ICLR)*, 2016.

Wesley J Maddox, Pavel Izmailov, Timur Garipov, Dmitry P Vetrov, and Andrew Gordon Wilson. A Simple Baseline for Bayesian Uncertainty in Deep Learning. In *Advances in Neural Information Processing Systems (NeurIPS)*, 2019.

Kevin P Murphy. *Machine Learning: A Probabilistic Perspective*, chapter 8.5 Online learning and stochastic optimization. MIT Press, 2012.

Maria-Elena Nilsback and Andrew Zisserman. Automated Flower Classification over a Large Number of Classes. In *2008 Sixth Indian Conference on Computer Vision, Graphics & Image Processing (ICVGIP)*, 2008.

Omkar M Parkhi, Andrea Vedaldi, Andrew Zisserman, and CV Jawahar. Cats And Dogs. In *Proceedings of the IEEE/CVF Conference on Computer Vision and Pattern Recognition (CVPR)*, 2012.

Adam Paszke, Sam Gross, Francisco Massa, Adam Lerer, James Bradbury, Gregory Chanan, Trevor Killeen, Zeming Lin, Natalia Gimelshein, Luca Antiga, Alban Desmaison, Andreas Kopf, Edward Yang, Zachary DeVito, Martin Raison, Alykhan Tejani, Sasank Chilamkurthy, Benoit Steiner, Lu Fang, Junjie Bai, and Soumith Chintala. PyTorch: An Imperative Style, High-Performance Deep Learning Library. In *Advances in Neural Information Processing Systems (NeurIPS)*, 2019.

Joelle Pineau, Philippe Vincent-Lamarre, Koustuv Sinha, Vincent Larivière, Alina Beygelzimer, Florence d'Alché Buc, Emily Fox, and Hugo Larochelle. Improving Reproducibility in Machine Learning Research (A Report from the NeurIPS 2019 Reproducibility Program). *The Journal of Machine Learning Research*, 22(1):7459–7478, 2021.

Ravid Shwartz-Ziv, Micah Goldblum, Hossein Souri, Sanyam Kapoor, Chen Zhu, Yann LeCun, and Andrew G Wilson. Pre-Train Your Loss: Easy Bayesian Transfer Learning with Informative Priors. In *Advances in Neural Information Processing Systems (NeurIPS)*, 2022. URL https://proceedings.neurips.cc/paper_files/paper/2022/file/b1e7f61f40d68b2177857bfcb195a507-Paper-Conference.pdf.

Martin Špendl and Klementina Pirc. [Re] Easy Bayesian Transfer Learning with Informative Priors. In *ML Reproducibility Challenge 2022*, 2023. URL https://openreview.net/forum?id=JpaQ8GFOVu.

Philipp Tschandl, Cliff Rosendahl, and Harald Kittler. The HAM10000 dataset, a large collection of multi-source dermatoscopic images of common pigmented skin lesions. *Scientific Data*, 5(1):1–9, 2018. URL https://dataverse.harvard.edu/dataset.xhtml?persistentId=doi:10.7910/DVN/DBW86T.

LI Xuhong, Yves Grandvalet, and Franck Davoine. Explicit Inductive Bias for Transfer Learning with Convolutional Networks. In *International Conference on Machine Learning (ICML)*, 2018.

Ruqi Zhang, Chunyuan Li, Jianyi Zhang, Changyou Chen, and Andrew Gordon Wilson. Cyclical Stochastic Gradient MCMC for Bayesian Deep Learning. In *Proceedings of the International Conference on Learning Representations (ICLR)*, 2019.

Fuzhen Zhuang, Zhiyuan Qi, Keyu Duan, Dongbo Xi, Yongchun Zhu, Hengshu Zhu, Hui Xiong, and Qing He. A comprehensive survey on transfer learning. *Proceedings of the IEEE*, 109(1):43–76, 2020.

A Classification

A.1 Dataset Details

Our experiments include a replication of CIFAR-10 (Krizhevsky et al., 2010) experiments from Shwartz-Ziv et al. (2022), similar Oxford Flowers (Nilsback & Zisserman, 2008) experiments to Shwartz-Ziv et al. (2022), similar Oxford-IIIT Pets (Parkhi et al., 2012) experiments to Shwartz-Ziv et al. (2022), and additional experiments on HAM10000 (Tschandl et al., 2018; Codella et al., 2019), a medical imaging dataset. For Oxford Flowers experiments, we modify prior experiments to enforce classes are uniformly distributed in the training data, that at least one sample from each class is included in the training data, and that the validation set is proportional with the training set. For Oxford-IIIT Pets experiments, we modify prior experiments to enforce classes are uniformly distributed in the training data, and that at least one sample from each class is included in the training data. For HAM10000 experiments, we form a classification task using classes with sufficient data (at least 10% prevalence) and an additional class including all other classes. For the validation set, we ensure each patient's data belongs to exactly one split and stratify by class to ensure comparable class frequencies. We use the same preprocessing steps for all four datasets.

Table A.1: Distribution of labels in HAM10000 training set.

Label	Percent of training set
Melanocytic	66.95%
Melanoma	11.11%
Benign keratosis	10.97%
Other	10.97%

For preprocessing, we use the mean and standard deviation of each channel from the training dataset of size n to normalize images. During fine-tuning we resize the images to 256x256 pixels, perform random cropping to 224x224, and horizontal flips. At test time, we resize the images to 256x256 pixels and center crop to 224x224.

A.2 Classifier Details

We use SGD with a Nesterov momentum parameter of 0.9 for optimization. We train for 6,000 steps using a cosine annealing learning rate (Loshchilov & Hutter, 2016). We select the initial learning rate from 4 logarithmically spaced values between 0.1 to 0.0001 and the weight decay from 5 logarithmically spaced values between $1e^{-2}$ to $1e^{-6}$, as well as without weight decay. For *LearnedPriorLR*, we select the covariance

scaling factor from 10 logarithmically spaced values between $1e^0$ to $1e^9$. While tuning hyperparameters, we hold out 1/5 of the training set for validation, ensuring classes are evenly distributed between sets. When the number of training samples is equal to the number of classes we validate on classes not in training data. After selecting the optimal hyperparameters from the validation set NLL, we retrain the model using the selected hyperparameters on both the training and validation images. Test results are reported.

StdPrior. Stocastic gradient descent (SGD) in PyTorch (Paszke et al., 2019) uses a modified gradient to add weight decay to the loss. If $\tau' > 0$ the optimizer updates $\nabla_w L_t(w_{t-1}) = \nabla_w L_t(w_{t-1}) + \tau' w_{t-1}$. This is equivalent to the following MAP objective

$$L(w, V) := -\frac{1}{n}\sum_{i=1}^{n} \log p(y_i|x_i, w) + \frac{\tau'}{2}||\text{vec}(V)||^2 + \frac{\tau'}{2}||w||^2. \tag{6}$$

The Bayesian interpretation of weight decay in PyTorch can be recovered with the Gaussian prior $\mathcal{N}(0, \tau I)$ where $\tau = \frac{1}{n\tau'}$. We use Shwartz-Ziv et al. (2022)'s SimCLR Resnet-50 pre-trained initialization to initialize weights w.

LearnedPriorIso. For *LearnedPriorIso*, we minimize the following MAP objective

$$L(w, V) := -\frac{1}{n}\sum_{i=1}^{n} \log p(y_i|x_i, w) + \frac{\tau'}{2}||\text{vec}(V)||^2 + \frac{\tau'}{2}||w - \mu||^2 \tag{7}$$

so that the weight decay search space is the same as SGD in PyTorch. We use Shwartz-Ziv et al. (2022)'s SimCLR Resnet-50 pre-trained initialization as the mean μ and to initialize weights w.

LearnedPriorLR. For *LearnedPriorLR*, we minimize the following MAP objective

$$L(w, V) := -\frac{1}{n}\sum_{i=1}^{n} \log p(y_i|x_i, w) + \frac{\tau'}{2}||\text{vec}(V)||^2 - \frac{1}{n}\log \mathcal{N}(w|\mu, \lambda\Sigma). \tag{8}$$

Although not discussed in Shwartz-Ziv et al. (2022), they add ε to the prior variance (they set the default value of ε to 0.1). We include the addition of ε to the prior variance by adding $\lambda\Sigma_{\text{diag}} + \varepsilon I$. We note that adding ε to the prior variance has a significant effect if the covariance scaling factor is small (e.g., $\lambda = 1$).

B Side-by-side Experimental Settings

Table B.1: A detailed comparison of Shwartz-Ziv et al. (2022)'s and our experimental procedures.

	Shwartz-Ziv et al. (2022)'s	**Ours**
Normalization	In their code, they use the mean and standard deviation of the entire training dataset.	We use the mean and standard deviation of the training dataset of size n.
Data augmentation	In their paper, they say they use random cropping and random horizontal flips. In their code, they use random vertical flips for some datasets as well.	We follow their paper, we use random cropping and random horizontal flips.
Batch size	They use a batch size of 128.	We use a batch size of 128.
Optimizer	They use SGD with a Nesterov momentum parameter of 0.9 for optimization.	We use SGD with a Nesterov momentum parameter of 0.9 for optimization.
Gradient clipping	In their paper, they do not mention gradient clipping. In their code, gradients are clipped so that the L2 norm is 2.0 by default.	We do not use gradient clipping. In our experiments, gradient clipping had little impact on performance.

Continued on next page.

Table B.1: Continued from previous page.

	Shwartz-Ziv et al. (2022)'s	**Ours**
Number of steps	For Bayesian inference they train for 30,000 steps using a cyclic learning rate (Zhang et al., 2019) with 5 chains. They never mention the number of steps they use for SGD-based methods.	We train for 6,000 steps using a cosine annealing learning rate (Loshchilov & Hutter, 2016) to reproduce their Bayesian inference settings for our SGD-based methods.
Initial learning rate	They select the initial learning rate from 7 logarithmically spaced learning rates between 0.1 and 0.0001.	We select the initial learning rate from 4 logarithmically spaced learning rates between 0.1 and 0.0001. We use a coarser search space to reduced computational complexity. We expect a finer search space to improve on our results.
Weight decay	They select weight decay from 7 logarithmically spaced values between $1e^{-6}$ and $1e^{-2}$, as well as without weight decay. They also divide weight decay by learning rate.	We select weight decay from 5 logarithmically spaced values between $1e^{-6}$ and $1e^{-2}$, as well as without weight decay. We do not divide weight decay by learning rate. We use a coarser search space to reduced computational complexity. We expect a finer search space to improve on our results.
Covariance scaling factor	In their paper, they plot test error on CIFAR-10 for 10 logarithmically spaced covariance scaling factors between $1e^0$ and $1e^9$ (see their Fig. 2d) but don't specify a search space for the hyperparameter. We assume they don't tune the covariance scaling factor since no search space is mentioned.	We select the covariance scaling factor from 10 logarithmically spaced values between $1e^0$ to $1e^9$.
Validation set size	In their paper, they don't say.	We use 1/5 of the training set.
Hyperparameter selection metric	In their paper, they don't say. In their code, they use loss.	We use the validation set NLL.
Rank of low-rank covariance	In their paper, they plot test error on CIFAR-10 and CIFAR-100 for covariance ranks between 0 and 9 (see their Fig. 2b) but use a rank of 5 for experiments.	We use a rank of 5 for experiments.
Prior epsilon (see App. A.2)	In their paper, they do not mention prior epsilon. In their code, the default is 0.1.	We use 0.1.

Continued on next page.

Table B.1: Continued from previous page.

	Shwartz-Ziv et al. (2022)'s	**Ours**
Double prior over weights w	In their paper, they say to add a zero-mean isotropic Gaussian prior over added parameters (e.g., classification head) to solve the target task. In their code, they use weight decay over all parameters.	We do not use weight decay over all parameters.
Covariance scaling	In their paper, they say to scale the covariance by multiplying $\lambda\Sigma$. In their code, they scale the covariance diagonal by multiplying $\lambda\Sigma_{\text{diag}}$ and the covariance factor by multiplying λQ which creates a multivariate normal distribution with covariance matrix $\lambda\Sigma_{\text{diag}} + \lambda^2\Sigma_{\text{LR}}$.	We scale the covariance factor by multiplying $\sqrt{\lambda}Q$ which creates a multivariate normal distribution with covariance matrix $\lambda\Sigma_{\text{diag}} + \lambda\Sigma_{\text{LR}}$.

C NLL Results

Table C.1: CIFAR-10 heldout NLL (lower is better) as target train set size n increases. For each method and train set size n, we ran our two-phase training pipeline (including hyperparameter tuning) on 3 distinct training sets (independent samples of n examples from the provided full training set). We report mean NLL on test set across these 3 trials, along with the min-max range. 10 classes, balanced. See App. A for details.

Method	n **= 10**	**100**	**1000**	**10000**	**50000**
StdPrior fromImgNet	2.47 (2.10-3.20)	1.48 (1.27-1.75)	0.71 (0.66-0.79)	0.23 (0.23-0.23)	0.11 (0.10-0.11)
LearnedPriorIso fromImgNet	2.31 (2.24-2.35)	1.40 (1.30-1.50)	0.68 (0.62-0.78)	0.18 (0.18-0.19)	0.09 (0.09-0.09)
LearnedPriorLR fromImgNet	2.69 (2.30-3.39)	1.31 (1.20-1.44)	0.58 (0.56-0.58)	0.22 (0.21-0.23)	0.10 (0.10-0.11)

Table C.2: Oxford Flowers heldout NLL (lower is better) as target train set size n increases. For each method and train set size n, we ran our two-phase training pipeline (including hyperparameter tuning) on 3 distinct training sets (independent samples of n examples from the provided full training set). We report mean NLL on test set across these 3 trials, along with the min-max range. 102 classes, balanced. See App. A for details.

Method	n **= 102**	**510**	**1020**
StdPrior fromImgNet	3.69 (3.40-4.23)	1.00 (0.96-1.05)	0.59 (0.58-0.61)
LearnedPriorIso fromImgNet	4.43 (3.62-5.14)	1.00 (0.96-1.03)	0.58 (0.57-0.59)
LearnedPriorLR fromImgNet	4.00 (3.59-4.81)	1.04 (0.95-1.14)	0.54 (0.52-0.58)

Table C.3: Oxford-IIIT Pets heldout NLL (lower is better) as target train set size n increases. For each method and train set size n, we ran our two-phase training pipeline (including hyperparameter tuning) on 3 distinct training sets (independent samples of n examples from the provided full training set). We report mean NLL on test set across these 3 trials, along with the min-max range. 37 classes, balanced. See App. A for details.

Method	n **= 37**	**370**	**3441**
StdPrior fromImgNet	3.33 (3.25-3.40)	1.78 (1.72-1.83)	0.59 (0.55-0.66)
LearnedPriorIso fromImgNet	3.62 (3.56-3.69)	1.79 (1.71-1.87)	0.58 (0.52-0.66)
LearnedPriorLR fromImgNet	3.62 (3.59-3.63)	1.69 (1.64-1.72)	0.52 (0.52-0.53)

Table C.4: HAM10000 NLL on heldout data (lower is better) as target train set size n increases. For each method and size n, we ran our two-phase training (including hyperparameter tuning) on 3 distinct training sets (independent samples of size n from the provided full training set). We report mean NLL on test set across 3 trials (min-max range). 4 classes, ranging from 11%-67% prevalance. See App. A for details.

Method	$n =$ **100**	**1000**
StdPrior fromImgNet	1.16 (0.91-1.33)	0.90 (0.79-1.00)
LearnedPriorIso fromImgNet	1.16 (0.91-1.32)	0.83 (0.79-0.91)
LearnedPriorLR fromImgNet	1.35 (0.89-1.90)	0.89 (0.78-1.09)

D Comparison of Fully-Supervised Pretraining

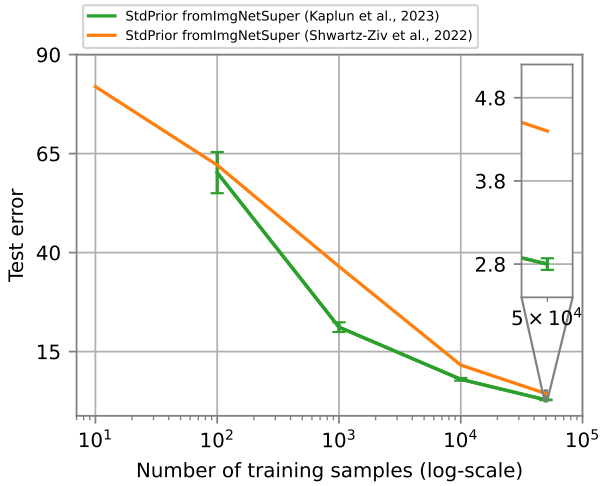

Figure D.1: Error rate (lower is better) vs. target train set size on CIFAR-10, for standard transfer learning from ImageNet using fully-supervised pre-training. The orange line are results copied from Shwartz-Ziv et al. (2022) (their Tab. 2). The green line is a third-party experiment copied from Kaplun et al. (2023). Plotted mean and standard deviations confirmed via direct correspondence with Kaplun et al.. **Takeaway: In third-party experiments, standard transfer learning performs better at dataset sizes** $n \in \{1000, 10000, 50000\}$ **than reported in Shwartz-Ziv et al. (2022).**

E Parameter Interpolation

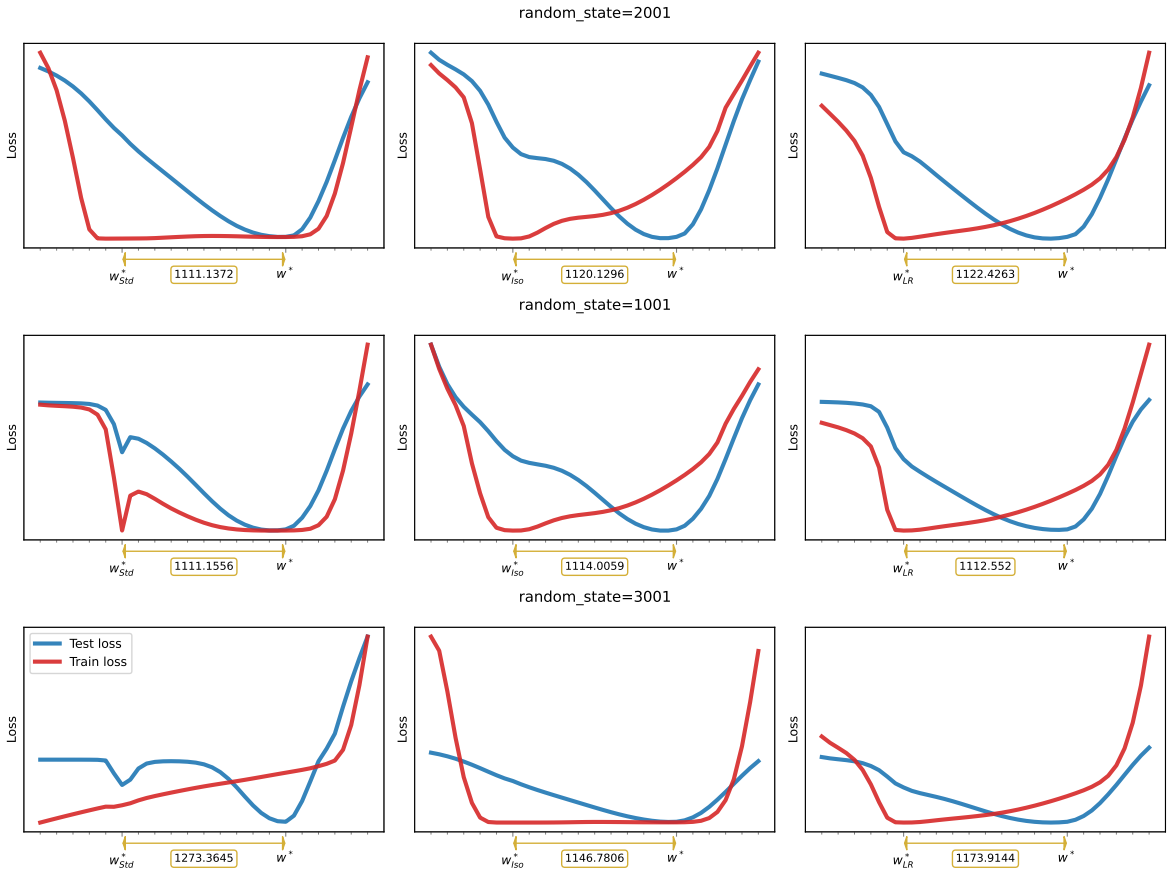

(a) Standard transfer learning (*StdPrior*) (b) *LearnedPriorIso* (c) *LearnedPriorLR*

Figure E.1: Empirical alignment of loss landscapes for target task across train and test for CIFAR-10 $n = 1000$. *Each panel:* We assess a 1D slice of the high-dimensional landscape by linearly interpolating parameters w between the optima w^*_{Std} found via minimizing the standard MAP objective (left), the optima w^*_{Iso} found via minimizing the *LearnedPriorIso* MAP objective (center), or the optima w^*_{LR} found via minimizing the *LearnedPriorLR* MAP objective (right) and the optima w^* found at the largest dataset size. Red curve shows the indicated training loss (varies by column) on CIFAR-10 with $n = 1000$ samples; blue curve (varies by column) shows CIFAR-10 test set NLL. Each row shows results from a different train set sample of size $n = 1000$. The gap between the optima found via training and the test set's ideal minimum is shown as a double-sided gold arrow.

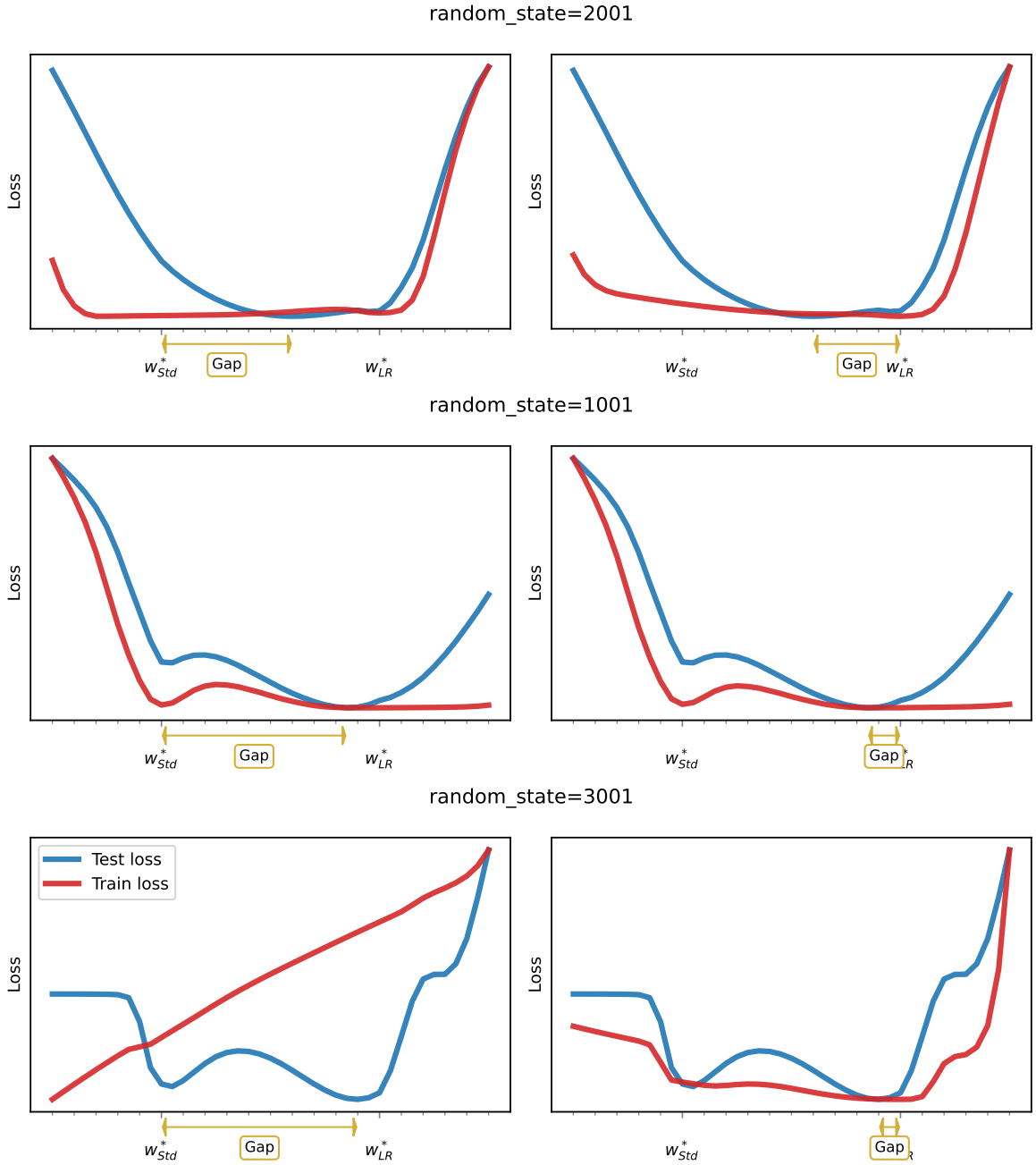

(a) Standard transfer learning (*StdPrior*)

(b) *LearnedPriorLR*

Figure E.2: Empirical alignment of loss landscapes for target task across train and test for CIFAR-10 $n = 1000$. *Each panel:* We assess a 1D slice of the high-dimensional landscape by linearly interpolating parameters w between the optima w^*_{Std} found via minimizing the standard MAP objective and optima w^*_{LR} found via minimizing the *LearnedPriorLR* MAP objective. Red curve shows the indicated training loss (varies by column) on CIFAR-10 with $n = 1000$ samples; blue curve (same across columns) shows CIFAR-10 test set NLL. Each row shows results from a different train set sample of size $n = 1000$. The gap between the optima found via training and the test set's minimum on the 1D slice is shown as a double-sided gold arrow.

F Comparison with Full Bayesian Inference

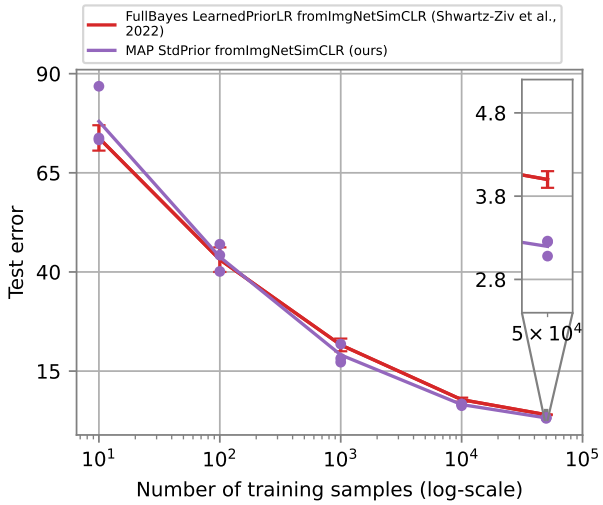

Figure F.1: Error rate (lower is better) vs. target train set size on CIFAR-10, for standard transfer learning and full Bayesian inference with *LearnedPriorLR* from ImageNet. The red line are results copied from Shwartz-Ziv et al. (2022) (their Tab. 10). **Takeaway: Our standard transfer learning results on CIFAR-10 are as good as or better than the full Bayesian inference results reported in Shwartz-Ziv et al. (2022).**

G Hyperparameter Sensitivity

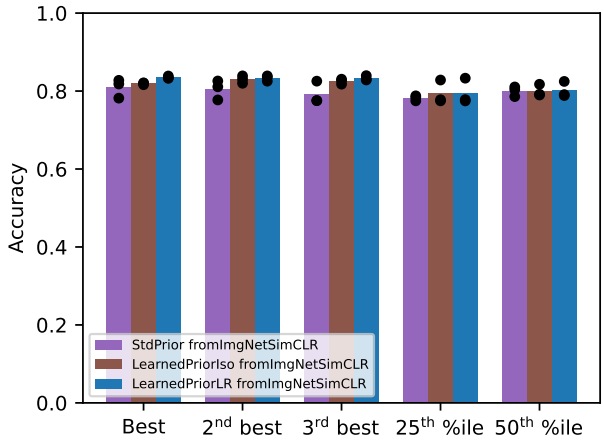

Figure G.1: Sensitivity of selected hyperparameters for CIFAR-10 $n = 1000$. We report CIFAR-10 heldout accuracy (higher is better) with various selected hyperparameters as validation NLL increases.